Mechanical Behavior of Tetrafunctional/Phenol Novolac Epoxy Mixtures Cured with a Diamine

L. BARRAL, J. CANO, J. LÓPEZ, I. LÓPEZ-BUENO, P. NOGUEIRA, M. J. ABAD, A. TORRES, C. RAMÍREZ

Departamento de Física, E. U. P. Ferrol, Universidad de A Coruña, Cra. Aneiros s/n, 15405 Ferrol, Spain

Received 6 May 1999; accepted 22 October 1999

ABSTRACT: An amine-cured epoxy system based on tetraglycidyldiaminodiphenylmethane and a novolac glycidyl ether resin was studied. Epoxies were prepared by varying the cure schedules and using the isothermal time–temperature–transformation diagram of the system. The materials were characterized using dynamic-mechanical analysis (DMA), tensile stress–strain tests over a range of temperatures and testing speeds, impact, and hardness tests. Optical microscopy was used to study the fracture surfaces of the samples. Some interrelations between the behavior and the microstructure of the system are discussed. In addition, the effect of thermal aging on the mechanical properties has been studied. DMA analysis seemed to reveal a structure that tended to be less heterogeneous with increasing the crosslink density. The advance in the etherification reactions or the thermal aging has reduced the mechanical properties related with the consumption of energy to break. The optimal cure schedule according to the global properties has been established. The morphology of fractured surfaces by optical microscopy showed a clear correlation with the variation of the tensile properties. © 2000 John Wiley & Sons, Inc. J Appl Polym Sci 77: 2305–2313, 2000

Key words: dynamic-mechanical analysis; epoxy resin; fractography; mechanical properties; time–temperature–transformation diagram

INTRODUCTION

Epoxy resins are important industrial polymers used in composite materials, adhesives, and coatings. The use in advanced composites is pressuring the advancement of epoxy science and the improvement of epoxy-based materials physical properties. The knowledge of thermomechanical and mechanical characteristics is necessary from an engineering viewpoint, and can be used to yield information on the microstructure of thermosetting resins.

The resin used in this study was a mixture of the epoxy prepolymers tetraglycidyl-4,4′-diaminodiphenylmethane and a novolac glycidyl ether resin, both cured with an aromatic amine hardener, the 4,4′-diaminodiphenylsulphone.

The cure kinetics and the construction of the isothermal time–temperature–transformation (TTT) diagram of this system have been studied previously.[1,2] The cure kinetics and the TTT diagram have been useful tools for designing and analyzing different curing processes.

In this paper, dynamic-mechanical and mechanical properties were studied with respect to the curing conditions, and some interrelations between the behavior and the microstructure of the system will be discussed. Moreover, the effect of thermal degradation on the properties has been investigated because this is a major problem in the application of these materials.

EXPERIMENTAL

Materials

The resin system used is a thermally cured epoxy consisting of MY720 and EPN 1138 epoxies, both

Correspondence to: L. Barral (E-mail: labpolim@udc.es).

Contract grant sponsor: Comision Interministerial de Ciencia y Tecnología; contract grant number: MAT97-0452.

Journal of Applied Polymer Science, Vol. 77, 2305–2313 (2000)

manufactured by Ciba-Geigy, and DDS amine curing agent, manufactured by Fluka Chemie. The MY720 is based on the prepolymer tetraglycidyl-4,4′-diaminodiphenylmethane (TGDDM). The EPN 1138 is a multifunctional novolac glycidyl ether resin, while DDS is the aromatic amine hardener, 4,4′-diaminodiphenylsulphone.

All these components were commercial products, and were used as received. The weights per epoxy equivalent for TGDDM and EPN were, respectively, 130 and 180 g eq^{-1}, obtained in our laboratory by hydrochlorination.[3] The weight composition of the mixture was 43.3% TGDDM, 35.7% EPN and 21.0% DDS, yielding an amine/epoxide ratio of 0.64.

An epoxy-rich formulation was chosen because of the significance of this kind of mixtures in the manufacture of high-performance composites. Thermal and mechanical properties of TGDDM/DDS systems have been studied in literature,[4–7] but there are few data of TGDDM/novolac/DDS systems.[8,9] Nevertheless, for optimum high-temperature properties, novolac epoxies should be considered.[10,11]

The thermosetting material was prepared by mixing the components at 120°C with continuous mechanical stirring, until a homogeneous liquid was reached. This mixture was poured into a rectangular stainless steel mold of 250 × 350 mm, which was preheated at the same temperature and placed into a forced air convection oven, where the curing schedules were applied. Finally, sheets of the cured material with slightly smaller dimensions than of the mold due to the shrinkage, and about 4 mm thick, were properly mechanized to obtain the samples for the different tests.

Dynamic-Mechanical Tests

Dynamic-mechanical analysis of cured samples measuring roughly 19 × 4 × 4 mm was performed between −100 and 300°C at several frequencies ranging from 0.1 to 30 Hz in three-point bending (i.e., flexural oscillation) using a Perkin Elmer DMA 7 analyzer equipped with a liquid nitrogen-cooling accessory CCA 7. The heating rate was 5 °C min^{-1}, under a helium flow of 40 cm^3 min^{-1}.

Mechanical Tests

Tensile stress–strain properties were measured according to general specifications of ASTM D638M and ISO 527, using an Instron universal-testing machine 5566 equipped with a climatic chamber Instron 3119-005. Tests were made at several temperatures and crosshead speeds. Samples were M-II type and a minimum of five of them was tested for each characterization. The data reported are averages of the results.

Charpy and Izod impact tests following ISO 179 and ISO 180 standards were made with an Instron Wolpert pendulum impact-testing machine PW5. The Izod pendulum had a potential striking energy of 50 J and the Charpy pendulum of 7.5 J, respectively. Unnotched type-I specimens according to the standards were used.

Rockwell hardness measurements were made with an Instron Wolpert hardness-testing machine DIA-TESTOR 722 following ASTM D785.

Finally, optical micrographs of the fracture surfaces were taken using a stereoscopic microscope Nikon SMZ-U, and changes in the mass of the specimens were measured on a Perkin Elmer AD4 balance having a resolution of 0.01 mg.

RESULTS AND DISCUSSION

Dynamic-Mechanical Properties and Curing Processes

The TTT diagram displaying the iso-conversion curves[2,12] was used to design three different curing paths (will be designated cure 1, 2, and 3) in order to obtain glassy solids which achieved an increased conversion.

The temperatures and time of the curing schedules were as follows: (cure 1) 120°C for 120 min followed by 170°C for 150 min; (cure 2) 180°C for 120 min; (cure 3) 160°C for 120 min and 220°C for 120 min.

Following the plots of the curing paths over the TTT diagram,[12] the material had reached increasing conversions ranging about 0.70 to 0.92 conversion curves. Transforming conversion values into glass transition temperature T_g values through the modified Di Benedetto equation used by Hale et al.,[13,14] from data obtained by differential scanning calorimetry (DSC) analysis,[2] we can expect values between 168 and 242°C for the T_g values of the material under the curing conditions selected, according to the range about 70–92% of conversion virtually reached.

Dynamic-mechanical tests were made for samples of the distinct cures, at the standard frequency of 1 Hz, using the temperature scan mode at a constant heating rate of 5°C min^{-1}. The main α relaxation, corresponding to the three-dimensional motion of chains and of crosslinking points

Table I Variation of the Properties of the System with the Curing Conditions

	Cure 1: 2 h at 120°C + 2.5 h at 170°C	Cure 2: 2 h at 180°C	Cure 3: 2 h at 160°C + 2 h at 220°C
T_g (°C)	172	211	251
E'_r (MPa)	24	35	73
h_α	0.67	0.41	0.29
E (MPa)	1636 ± 19	1499 ± 32	1705 ± 37
σ_B (MPa)	65 ± 12	64 ± 4	54 ± 8
ε_B (%)	5.0 ± 1.0	6.2 ± 0.7	4.0 ± 0.9
Toughness (MPa)	1.8 ± 0.7	2.2 ± 0.4	1.2 ± 0.5
Rockwell hardness E	90.4 ± 0.5	91.0 ± 1.3	84.0 ± 0.8

during the glass–rubber transition process, was clearly observed.

From the dynamic-mechanical tests, several parameters have been determined for the glass transition region: the glass transition temperature T_g, the height of the damping peak h_α and the rubber plateau storage modulus E'_r, taken at T_g +40°C. The temperatures corresponding to the maximum in tanδ curves on the α relaxation were taken as the T_g values.

Table I lists the values of these parameters and summarizes the cure conditions.

The good agreement between the experimental DMA T_g values and the expected values made on the basis of the TTT diagram and the one-to-one relationship between T_g and conversion of the empirical Di Benedetto equation can be appreciated, taking into account the differences between data obtained by DSC and DMA techniques.

The increasing values of T_g and E'_r from cure 1 to cure 3, so as the decrease in the heights of tanδ peaks, are related to the advance in the extension of the curing reactions, which have increased the crosslink density of the epoxy and restricted the mobility of the chains.[15]

From Table I, T_g value of cure 1, 172°C, is practically the final curing temperature for this path. T_g values are 30°C above their final curing temperatures for cures 2 and 3. The previous work about cure kinetics[1] showed that at the point where vitrification slowed down the reaction significantly, the epoxide amine reaction was virtually complete, regardless of temperature, but the epoxide-hydroxyl reaction was only partially complete.

From 210°C, etherification reactions became more significant with increasing temperature, e.g., at a curing temperature of 230°C, 62% of the epoxide groups have reacted with amine, 14% have reacted with OH and 24% remain unreacted, for the material having vitrified.

Thus, in this epoxy-rich system, etherification is an important fact that contributes to the increase in the crosslinking of the network, even after having vitrified the material. Because of the rate of these reactions is low, the time and the high temperatures could significantly impact the final T_g of the samples,[16,17] as was observed.

Multifrequency DMA Analysis

The influence of frequency on the dynamic-mechanical behavior of the cure 1 and cure 3 systems is presented in Figures 1 and 2. These curing paths were selected in this analysis for being the ones corresponding to the minimum and the maximum conversion, respectively.

An Arrhenius-type relationship was used to fit the data obtained for the temperatures of the maximum peaks in tanδ, for several frequencies. A graph of the applied log (frequency) against the inverse of the absolute temperature corresponding to the maximum on the α relaxations yields the activation energies from the slope of the straight line fitting the data. Values of 300 and 677 kJ mol^{-1} were obtained for cure 1 and 3, respectively.

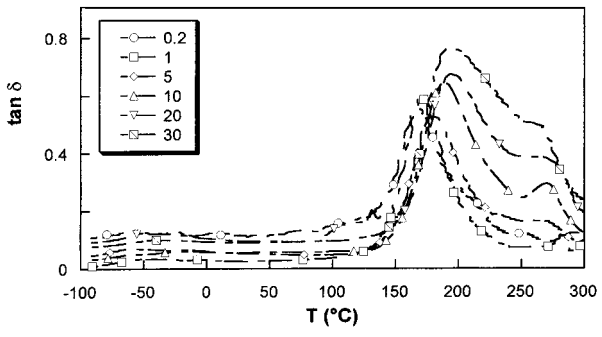

Figure 1 DMA curves for several frequencies (Hz) for cure 1.

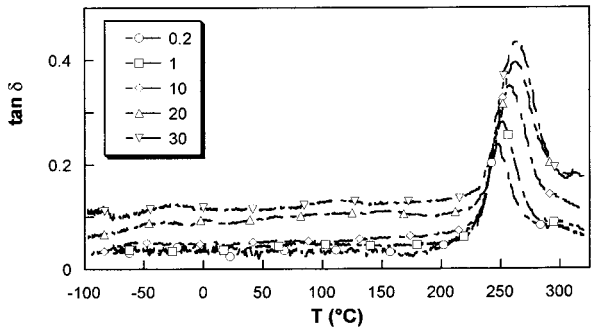

Figure 2 DMA curves for several frequencies (Hz) for cure 3.

The higher activation energy for the α relaxation in cure 3 is attributed to the greater extension of the curing reactions, i.e., the higher crosslinked network.

Both the T_g values and the heights of the damping peaks increase with frequency, but in cure 1 this behavior is not so regular, and a shoulder or second peak appeared above the maximum with increasing frequency, c.a., 266°C, precisely the glass transition temperature of the fully reacted material $T_{g\infty}$, calculated in a previous study.[2]

These secondary peaks are not observed in cure 3, so we can relate them with the existence of a more heterogeneous network in the material with a lesser conversion.

Several researchers have reported the existence of a heterogeneous network in epoxy–amine systems. The studies of Keenan et al. and Stark et al.[18,19] on a TGDDM/DDS system with a novolac of high functionality showed that regions of both high and low crosslink density existed due to the presence of two different epoxides, the processing conditions employed, the various types of reactions, as well as diffusional and steric factors. Recently, Vanlandingham et al.[20] have employed DMA analysis, density measurements, and atomic force microscopy (AFM) to investigate the structure of amine-cured epoxy systems. Phase and topographic AFM images exhibited a two-phase structure consisting of a hard microgel phase and a dispersed phase of soft, unreacted, and/or partially reacted material.

Thus, the secondary damping peaks could be the manifestation in DMA tests of regions of highly crosslinked material in the soft phase of the system under cure 1, which turned out to be more significant with increasing frequency, i.e., shorter relaxation times. The advance in the curing reactions determined a less heterogeneous structure of a progressively more crosslinked network. Finally, the glass transition of the main, high crosslinked phase was shown in the prominent single peak in the region of temperatures near $T_{g\infty}$, for cure 3.

Mechanical Properties

Tensile properties such as tensile stress at break (σ_B), percent elongation at break (ε_B), tensile modulus (E), and tensile toughness, calculated as the area under the stress–strain curve and representing the tensile energy absorption, were determined from stress–strain tests.

The average values of these properties with their standard deviations are reported in Table I. No yield points were observed, so the tensile strength is the same as σ_B.

In Figure 3 we have plotted the stress–strain average curves obtained at different temperatures using the climatic chamber with the universal-testing machine, for the material under cure 2. Figure 4 displays the variation of the tensile properties of cure 2 with the speed of testing.

Both the temperature and the rate of strain may affect dramatically the mechanical properties, and is necessary to consider them in order to get useful information for engineering purposes. The material under cure 2 has been chosen as reference for the detailed study of the mechanical properties due to its superior strength, toughness, and elongation at break.

From the data obtained for the different cures, it can be observed a better global behavior of cure 2, which had the lowest modulus and the highest toughness. Cure 3 presented the highest modulus but the lowest toughness. The unexpected increase in the fragility of the material with the

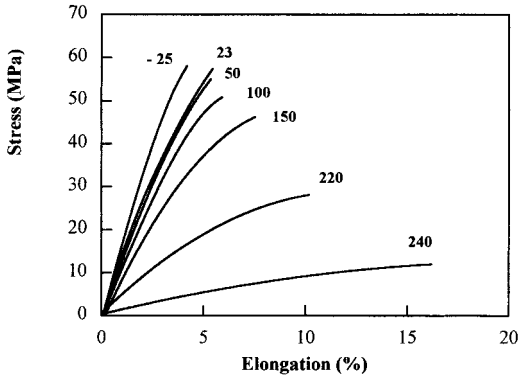

Figure 3 Influence of the temperature (°C) on the tensile behavior.

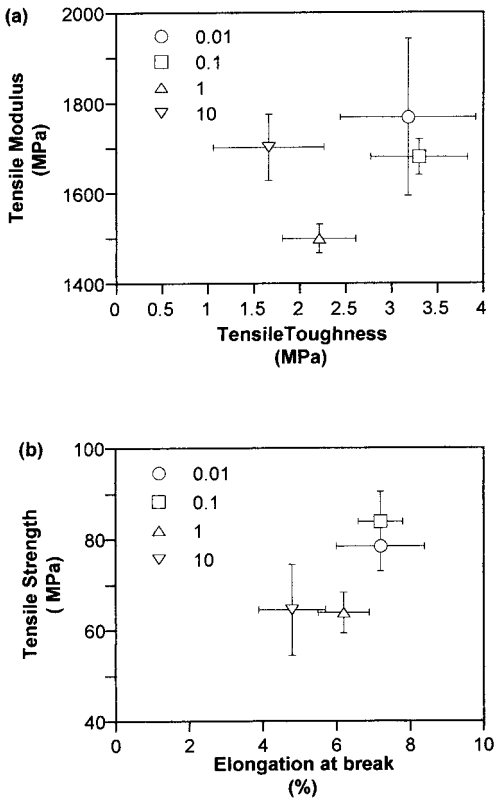

Figure 4 Tensile properties and their variation with the testing speed (mm/min): (a) elastic modulus and toughness and (b) strength and elongation at break.

increase in cure temperature may be due to etherification reactions arising from the cure at superior temperatures. In fact, side reactions like etherification change the structure of the networks by the formation of additional crosslinks of the ether type. This effect may be really pronounced in nonstoichiometric systems with an excess of epoxy components. So, for cure 3, the high temperature curing treatment has caused an activation of the etherification reactions, which determined a rise of the experimental T_g value and an increase in the Young modulus, but the material became more brittle, diminishing the toughness. This behavior has been found by other authors.[21]

Also, the stiffness was increased with increasing testing speed, decreasing the tensile strength, the elongation at break and the toughness, as showed data plotted in Figures 4(a) and (b).

The increase in the temperature produced a continuous decrease in the moduli (calculated over the initial slope of the curves) and in the strength; e.g., at 240°C tensile modulus was just 10% of ambient modulus, and tensile strength over 20% of ambient strength.

The greater variation in the properties occurred as the temperature was approaching to the T_g of the material. The tensile behavior was that of a highly crosslinked system that increased relatively the elongation at break but within a brittle behavior. Both elastic modulus E and dynamic storage modulus E' diminished one order of magnitude from the glassy to the rubbery state.

Optical micrographs of the fracture surfaces in Figure 5, with 2.5× photographic magnification, revealed important changes with temperature.

Figure 5(d) shows the four zones of the failed surfaces as highlighted in the work of Cantwell et al.[22]: a defect, a smooth mirror-like region of slow crack growth; a smooth region where the crack accelerates in an unstable manner and a rough three-dimensional area where the crack achieved its limiting velocity and produced multiple fracture surfaces.

The more brittle behavior at lower temperature is observed in Figures 5 (c) and (d), where the crack rapidly reached the maximum velocity and multiple fracture surfaces in the extensive rough areas appeared.

At high temperatures, the material showed their maximum values of elongation and the lowest moduli. This lower stiffness is seen in the surfaces of Figures 5(a) and (b), where the rough zones have disappeared suggesting that crack had either stabilized at a velocity below the limiting value or else that required acceleration zone was larger than the specimen dimensions.

Charpy impact strength a_{cu} and Izod impact strength a_{iu} at room temperature in unnotched specimens type-I were calculated from the tests made using the Instron Wolpert pendulum impact-testing machine PW5. Direction of blow was edgewise in Charpy tests and flat-wise in Izod tests.

Data obtained are shown with their standard deviations in Figure 6. A comparison of the Charpy impact strength with the tensile toughness for the different cures is shown in Figure 7.

The usual low impact strength of highly crosslinked thermosets was observed. However, the cure 2 exhibited both the highest impact strength and tensile toughness, being measurements of the consumption of energy at break.

Rockwell hardness has been evaluated at room temperature. Rockwell hardness number is directly related to the indentation hardness of a plastic material, with the higher the reading the harder the material. ASTM D785 procedure A, with fully specified time scales, has been selected, since the control of the time scale (e.g., rate of

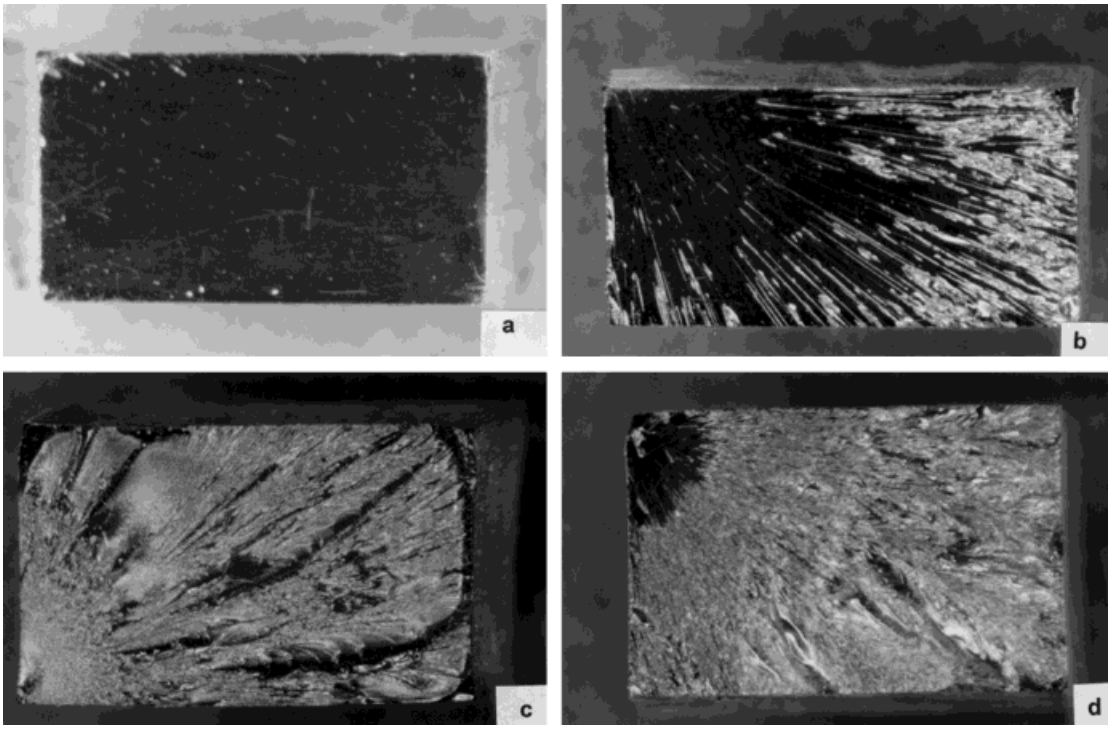

Figure 5 Optical micrographs of the fracture surfaces at (a) 240, (b) 220, (c) 50, and (d) −25°C.

loading and time after loading at which the reading is taken) is essential due to the viscoelastic response of the material.[23] Results obtained in Rockwell E scale (980 N of major load and 98 N of minor load with an indenter diameter of 3.175 mm) are presented in Table I.

The lowest indentation hardness was observed in cure 3. The better behavior in several properties of cure 2, and the loss of properties in cure 3, revealed a nonlinear correspondence between the mechanical response of the material and the extent of reaction. The changes in the structure of the network for both curing paths occurred after essentially all the epoxy–amine reactions were completed. Thus, etherification reactions in the highest temperature path have been a factor that has increased the stiffness of the material, reducing the properties at break.

Influence of Thermal Aging

The exposure to high service temperatures is a common fact in the application of these materials.

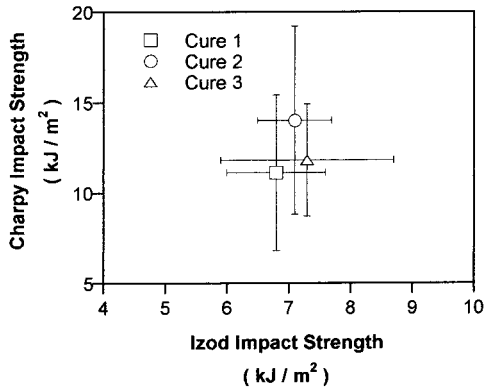

Figure 6 Charpy and Izod impact strength of the different cures.

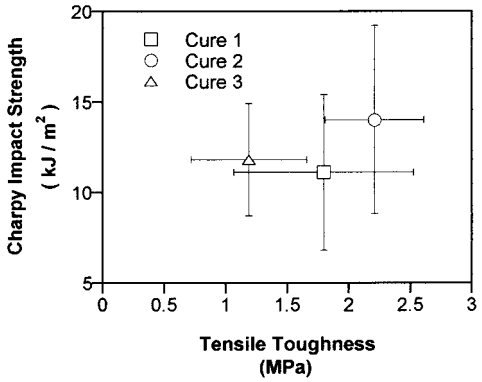

Figure 7 Measurements of energy absorption at break.

Table II Influence of Thermal Aging on Some Properties of the System

	Exposure Time (h)			
	0	24	96	240
Loss of mass (%)	0	1.0	2.0	3.1
T_g (°C)	211	246	258	248
E'_r (MPa)	26	42	78	51
h_α	0.41	0.28	0.32	0.31
Rockwell hardness E	91.0 ± 1.3	98.6 ± 1.7	99.0 ± 0.9	101.2 ± 1.5

The variation of the properties for the material with the optimum balance in the properties, cure 2, has been studied as a function of the time of exposure to a temperature of 200°C, near its T_g.

The values of the dynamic mechanical parameters and the average loss of mass for several specimens after 0, 24, 96, and 240 h of thermal aging time at 200°C are shown in Table II. Dynamic-mechanical tests were made under the same conditions than initial characterization.

Results in Table II may be explained based on an initial reactivation of the crosslinking reactions, which increased T_g and the rubbery modulus E'_r, decreasing the height of tanδ peaks. This could be possible since the material had not reached the maximum conversion, and more than 25% epoxy groups remained unreacted. Also, other reactions than epoxy–amine have contributed to this increase in the effective crosslink density.

After an initial period, thermal degradation has caused structural losses in the material, breaking crosslink points, losing dangling chains, decreasing the effective crosslink density, and reducing E'_r and T_g values. The increase in mobility of the macromolecular chains in the glass transition region can be appreciated in the increase of the height of tanδ peaks respect to the first thermal aging values.

Stress–strain tests on specimens subjected to the same aging temperature and time were made to study the variation on the mechanical properties. The average values with their deviations are represented in Figure 8. The material increased the stiffness, with higher elastic moduli and decreasing the properties at break.

Optical micrographs in Figures 9(a) and (b) of fracture surfaces, with 0 and 96 h of thermal aging time respectively, showed a large three-dimensional area of brittle fracture with 96 h of exposure at 200°C, compared with the less prominent structures for the nonaged material. Etherification, oxidation, or another degradative reactions also could be responsible for the color changes to a dark brown of these epoxy-rich specimens with aging time.

Rockwell hardness results are given in Table II. The indentation strength has been increased with aging time. This fact, and the increase in the tensile moduli, is related with the more rigid, brittle behavior of the system after the exposure at relatively high temperature.

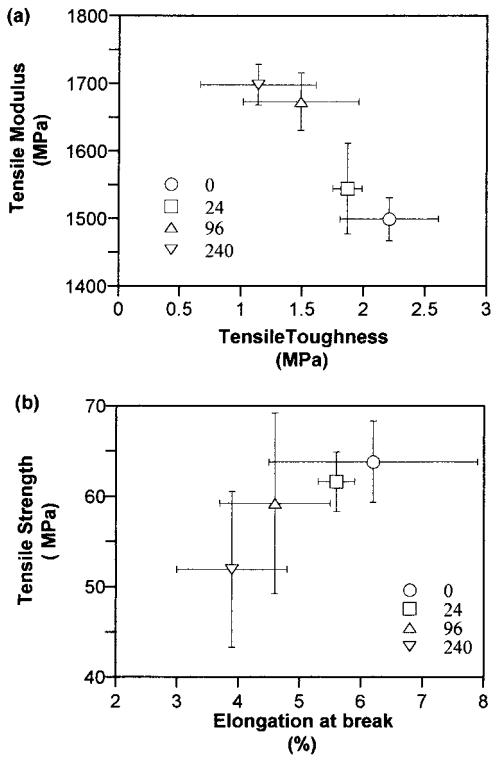

Figure 8 Variation of the tensile properties with thermal aging time (h): (a) elastic modulus and toughness and (b) strength and elongation at break.

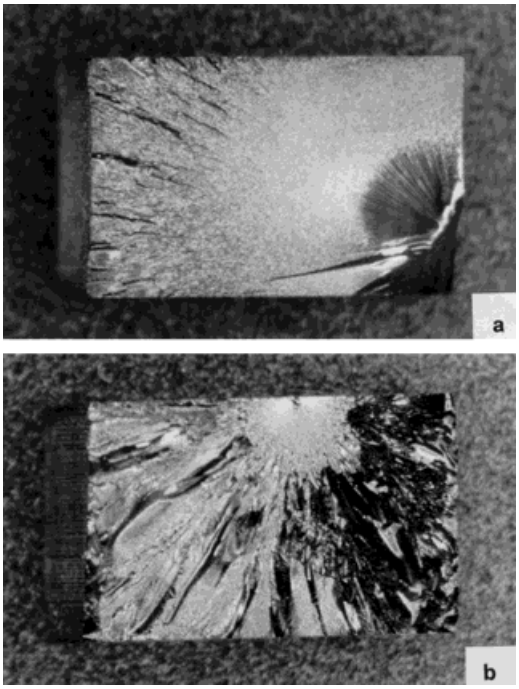

Figure 9 Tensile fracture surfaces of: (a) the nonaged material and (b) with 96 h of thermal aging time.

CONCLUSIONS

Different curing paths have been designed for a TGDDM/EPN/DDS epoxy system on the basis of the previous knowledge of the cure kinetics and the TTT diagram of this system.[1,2] Previsions about the degree of conversion reached following the plots of the curing schedules over the TTT diagram were in good agreement with T_g values obtained using DMA analysis and correlated with conversion through a modified Di Benedetto equation by Hale et al.[14] This fact confirmed the TTT diagram as an useful tool to design curing processes in order to obtain a material with some expected properties.

Depending on the extent of the crosslinking reactions, different structures in the system, as related by some authors,[18–20] could be inferred from the DMA analysis. For cure 1, the structure seemed to be heterogeneous, with a phase of highly crosslinked material and a phase of unreacted and/or partially reacted material. The structure tended to be less heterogeneous with the increase in the network crosslinking.

Since epoxy–amine reactions were virtually completed for the conversions reached, another kind of reaction has contributed to the increase in the effective crosslink density showed in T_g and E'_r values. The main one was a epoxy-hydroxyl or etherification reaction, taken into account in the cure kinetics of the system. These reactions became more important as the temperature of the curing processes was raised, and with the exposure of the partially cured material to high temperatures.

Tensile stress–strain, impact and hardness measurements have been made, and the optimum balance in the mechanical properties was obtained for the material cured 2 h at 180°C, which presented better properties at break at any aging time.

Thermal degradation and/or the advance of the etherification reactions reduced the mechanical properties related with the energy consumption to break. In this way, curing at high temperatures (above 200°C) must be avoided in order to reduce the losses of the properties in this system.

The morphology of fractured surfaces by optical microscopy showed a clear correlation with the variation of the tensile properties.

REFERENCES

1. Barral, L.; Cano, J.; López, J.; Nogueira, P.; Abad, M. J.; Ramírez, C. J Therm Anal 1997, 50, 409.
2. Barral, L.; Cano, J.; López, J.; Nogueira, P.; Ramírez, C.; Abad, M. J. Polym Int 1997, 42, 301.
3. Jahn, H.; Goetzky, P. In Epoxy Resins, Chemistry and Technology; May, C. A., Ed.; Marcel Dekker: New York, 1988; Chap 13.
4. Mijovic, J.; Kim, J.; Slaby, J. J Appl Polym Sci 1984, 29, 1449.
5. Barton, J. M. Br Polym J, 1986, 18, 37.
6. Morgan, R. J.; Mones, E. T. J Appl Polym Sci 1987, 33, 999.
7. Chiao, L. Macromolecules 1990, 23, 1286.
8. Stark, E. B.; Ibrahim, A. M.; Seferis, J. C. In Interrelations between Processing Structure and Properties of Polymeric Materials; Seferis, J. C., Theocaris, P. S., Ed.; Elsevier: Amsterdam, 1984; p 23.
9. Cole, K. C.; Hechler, J. J.; Noel, D. Macromolecules, 1991, 24, 3098.
10. Oyanguren, P. A.; Williams, R. J. J. J Appl Polym Sci 1993, 47, 1361.
11. Lee, S. M. In Epoxy Resins, Chemistry and Technology; May, C. A., Ed., Marcel Dekker: New York, 1988; Chap 9.
12. Nogueira, P. Ph.D. thesis, Universidad de Santiago, 1998.
13. Nielsen, L. E. J Macromol Sci Rev Macromol Chem 1969, 3, 69.
14. Hale, A.; Makoso, C. W.; Bair, H. E. Macromolecules 1991, 24, 2610.
15. Ellis, B.; Found, M. S.; Bell, J. R. J Appl Polym Sci 1996, 59, 1493.

16. Zukas, W. X. J Appl Polym Sci 1994, 53, 429.
17. Simon, S. L.; Gillham, J. K. J Appl Polym Sci 1994, 53, 709.
18. Keenan, J. D.; Seferis, J. C.; Quinlivan, J. T. J Appl Polym Sci 1979, 24, 2375.
19. Stark, E. B.; Ibrahim, A. M.; Seferis, J. C. 28th National SAMPE Symposium 1983, 581.
20. Vanlandingham, M. R.; Eduljee, R. F.; Gillespie, J. W., Jr. J Appl Polym Sci 1999, 71, 699.
21. Oleinik, E. F. In Epoxy Resins and Composites IV; Dusek, K., Ed.; Springer-Verlag: Berlin, 1986; p 75.
22. Cantwell, W. J.; Kausch, H. H. In Chemistry and Technology of Epoxy Resins; Ellis, B., Ed.; Chapman and Hall: London, 1993; Chap 5.
23. Nielsen, L. E.; Landel, R. F. In Mechanical Properties of Polymers and Composites; Marcel Dekker: New York, 1994, Chapter 5.